Quaternary evolution of the inner Riss Valley, Tyrol (Austria) – an integrated sedimentological and geophysical case study

David MAIR[1] [*)], Werner CHWATAL[2)], Paula J. REIMER[3)] & Christoph SPÖTL[4)]

[1)] Institute of Geology, University of Innsbruck, Innrain 52, 6020 Innsbruck, Austria; Present address: Institute of Geological Sciences, University of Bern, Baltzerstrasse 1+3, 3012 Bern, Switzerland;

[2)] Department of Geodesy and Geoinformation, TU Wien, Gusshausstr. 27-29, 1040 Vienna, Austria;

[3)] Centre for Climate, the Environment and Chronology (14CHRONO), School of Natural and Built Environment, Queen's University Belfast, Belfast BT7 1NN, UK;

[4)] Institute of Geology, University of Innsbruck, Innrain 52, 6020 Innsbruck, Austria;

[*)] Corresponding author: david.mair@geo.unibe.ch

Abstract

We present the results of a study examining Quaternary sediments in the central and inner Riss Valley of the Karwendel Mountains, Tyrol. By using geological mapping, seismic and geoelectrical surveys, as well as shallow drilling and radiocarbon dating we investigated the sedimentary evolution of this previously poorly studied area. At Großer Ahornboden, seismic data reveal a glacially carved bedrock surface, buried beneath up to 140 m of sediments. The lowest sediment sequence consists of consolidated sediments showing high seismic velocities (2750 m/s) and reaching a thickness of 115 m. The overlying uncompacted sequence yielded lower velocity values (500 to 1100 m/s) and is interpreted as Holocene valley fill, with sediment derived from Rissbach river, small talus screes and debris-flow fans from tributary creeks. Up to 10-m-thick deposits of a Holocene paleolake, dammed by a large Lateglacial terminal moraine ridge, are present at the northern rim of Großer Ahornboden. Radiocarbon dates constrain the duration of this lake to between 10.5-10.2 and 5.5-5.3 cal ka BP. Lacustrine sediments pinch out in the subsurface just below the small fan leading down from Tränkkarl. In the central Riss Valley over 100 m thick, consolidated sediments of a proglacial delta are exposed. This delta complex consists of bottomset silts and thick foreset gravel and is overlain by diamict forming poorly developed moraine ridges of Lateglacial origin.

Die vorliegende Arbeit präsentiert eine Studie quartärer Sedimente des mittleren und inneren Risstales im Karwendelgebirge in Tirol. Mithilfe von geologischer Kartierung, seismischen Untersuchungen, Widerstandsgeolektrik, Rammkernsondierung sowie Radiokarbondatierung wird die Sedimentationsgeschichte des bisher spärlich untersuchten Gebietes beleuchtet. Im Bereich des Großen Ahornbodens offenbaren die seismischen Daten eine bis zu 140 m tief unter Sedimenten begrabene, glazial geformte Felsoberfläche. Die tiefsten, bis zu 115 m mächtigen, konsolidierten Sedimente weisen hohe seismische Wellengeschwindigkeiten (2750 m/s) auf. Die überlagernden, nicht verfestigten Sedimente zeigen deulich geringere Geschwindigkeiten (500 – 1000 m/s) und werden als holozäne Talfüllung gedeutet, die durch den Rissbach in Verbindung mit Schuttkegeln sowie durch lokale Schwemmfächer gebildet wurde. Bis zu 10 m mächtige holozäne Seesedimente finden sich am Nordrand des Großen Ahornbodens, direkt südlich einer spätglazialen Endmoräne, die als Damm des Paläosees fungierte. Radiokarbondatierungen erlauben die zeitliche Einordnung dieser Seephase zwischen 10,5-10,2 und 5,5-5,3 kal ka BP. Die lakustrinen Silte lassen sich nach Süden verfolgen bevor sie im Untergrund im Bereich des kleinen Schwemmfächers unterhalb des Tränkkarls auskeilen. Im zentralen Risstal ist eine verfestige, mehr als 100 m mächtige kaltzeitliche Deltaabfolge bestehend aus Silten (bottomset) und Kiesen (foreset) aufgeschlossen. Diese wird überlagert von einem spätglazialen Diamikt und schlecht erhaltenen Moränenwällen.

1. Introduction

The Pleistocene glaciations profoundly shaped the surface of the Alps, creating steep topographies and trough-shaped and commonly overdeepened valleys. Vast amounts of clastic sediment were deposited, eroded and redistributed. Major pulses of sediment accumulation and valley-floor aggradation were triggered by climate cooling, lowering of the equilibrium line altitude, expanding permafrost, intensifying frost shattering and lowering of the treeline. During glacial periods a wedge of sediments prograded from the inner alpine valleys into the foreland of the Alps fed by the advancing glaciers (van Husen, 2000; Hinderer, 2001). This led to a rise of the inner alpine

valley floors, locally enhanced by damming by sediment fans and/or glacier tongues from tributaries joining the main valleys. For example, the central Inn Valley in Tyrol was some 250 m higher at the end of the Middle Würmian some 30 ka ago and the river valley was two to three times wider than today (Spötl et al., 2014). The Last Glacial Maximum (LGM) resulted in large-scale erosion of these former sediments, whereby the depth of this subglacial erosion is poorly known in most valleys of the Alps (Preusser et al., 2010). Subsequent to the LGM large quantities of clastic sediment were deposited during the meltdown of the ice masses (Reitner et al., 2010). This
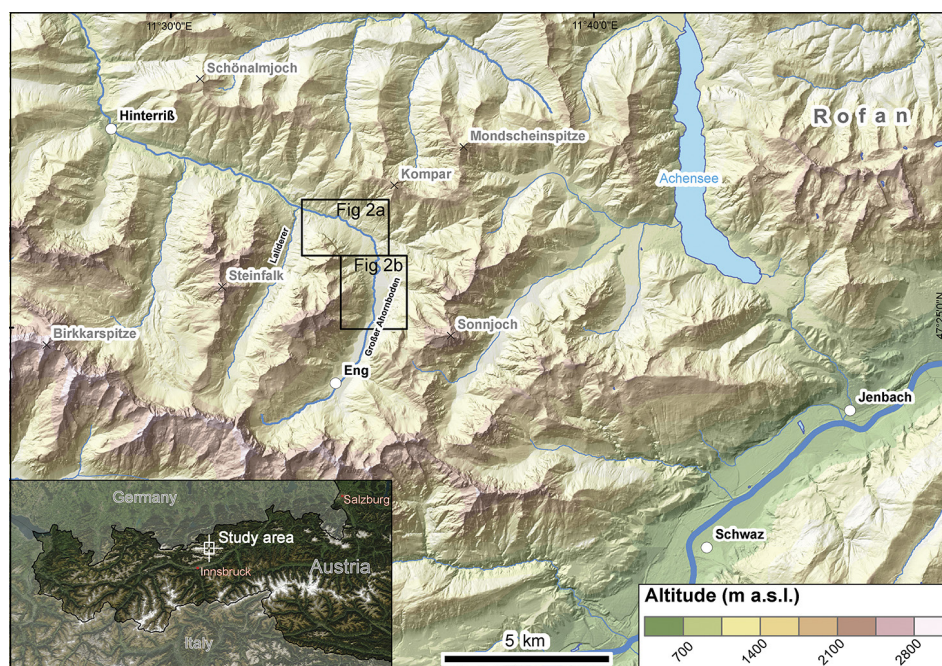
Figure 1: Regional map of the study area in the Karwendel Mountains in the western part of Austria. Basemap: digital elevation model by TIRIS (Source: Land Tirol - data.tirol.gv.at, ©CC BY 3.0 AT).

3. Methods

Sediments in the northern part of the study area, from Karlgraben to Hagelhütte (Fig. 2a), are well exposed along the Rissbach and its tributaries and were mapped and logged. In the southern part, leading to Großer Ahornboden, only limited and shallow outcrops exist. This area was studied using a combination of seismic surveys and percussion coring (Schrott and Sass, 2008).

3.1 Mapping and logging

The sediments were mapped at a scale of 1:5,000, aided by laser scan images (raster cell size 1x1 m; provided by tiris). Sediment logging of the well-exposed outcrops allowed the identification of several distinct lithofacies types (A to F) which can be correlated to sediments in the northern Riss Valley (Spötl et al., 2014).

3.2 Shallow coring and sampling

Percussion coring was used to obtain sediment cores down to a depth of 17 m in the area of Großer Ahornboden (DS in Figs. 2a and 2b). Although this technique causes sediment compaction up to about 10% of the core length (which was corrected for) and sediment disturbance near the flanks of the cores it provides direct access to sediments in the shallow subsurface. Discrete wood samples for radiocarbon dating were only taken from the inner, least disturbed part of the cores.

3.3 Grain-size analysis

Grain sizes of the sandy and finer sediments were determined by wet sieving. A laser particle analyzer (Malvern Instruments Mastersizer 2000 with a Hydro 2000MU pump) was used to determine the grain-size distribution of the <2 mm fraction. Each measurement comprised three separate measurements with 1000 readings (snaps) per second each leading to a total of 36,000 snaps, which were averaged. Sample preparation, pump speed (1900 rpm), obscuration (between 15 and 20%) and ultrasonic application (10 µm displacement for 60 s) followed the recommendations by Sperazza et al. (2004) for fine grained sediments and yielded results with ~5% uncertainty (2σ).

3.4 Radiocarbon dating

Wood samples obtained both from natural outcrops and percussion cores were prepared at the [14]CHRONO Centre, Queen's University Belfast, and analyzed using acceleration mass spectrometry (AMS). MIS 7 kauri wood (Hogg et al., 2006) provi-

was followed by several lateglacial glacier re-advances, which, however, were confined to the interior parts of the Alps. Finally, erosion and sedimentation during the Holocene have been largely controlled by the interplay between alluvial fans and the main rivers.

Here, we report an example of a major tributary valley in the Northern Calcareous Alps of Austria where an unusually well-exposed sediment-fill is preserved. Using a combination of field mapping, sediment logging, shallow coring as well as geophysical methods we attempt to unravel the dynamic Late Pleistocene landscape evolution of this part of the Eastern Alps.

2. Geological Setting

The study area is located in the inner Riss Valley of the Karwendel Mountains, Tyrol. It reaches from the Eng, the innermost part of the valley in the southeast, to the junction with the Laliderer tributary valley in the northwest (Fig. 1). The Riss Valley is deeply incised and runs from south to north in the southern part, where a conspicuously wide and nearly flat valley floor (Großer Ahornboden) is flanked by steep bedrock walls, and follows a northwestern direction in the northern part. South of Eng the impressive north face of the Karwendel Mountains rises up 2600 m a.s.l. The transition between the two valley morphologies roughly coincides with the tectonic boundary between the Lechtal and Inntal nappes which crosses the valley in E-W direction in the region of Hagelhütte (Fig 2). Quaternary deposits form sediment bodies of up to 140 m in thickness along the inner Riss Valley. The sediments show distinctive lithofacies types, which can be traced laterally and are well exposed. The presence of these sediments has been known since many decades (Ampferer, 1903; Wolf, 1922; Mutschlechner, 1948), but they have never been studied in detail.
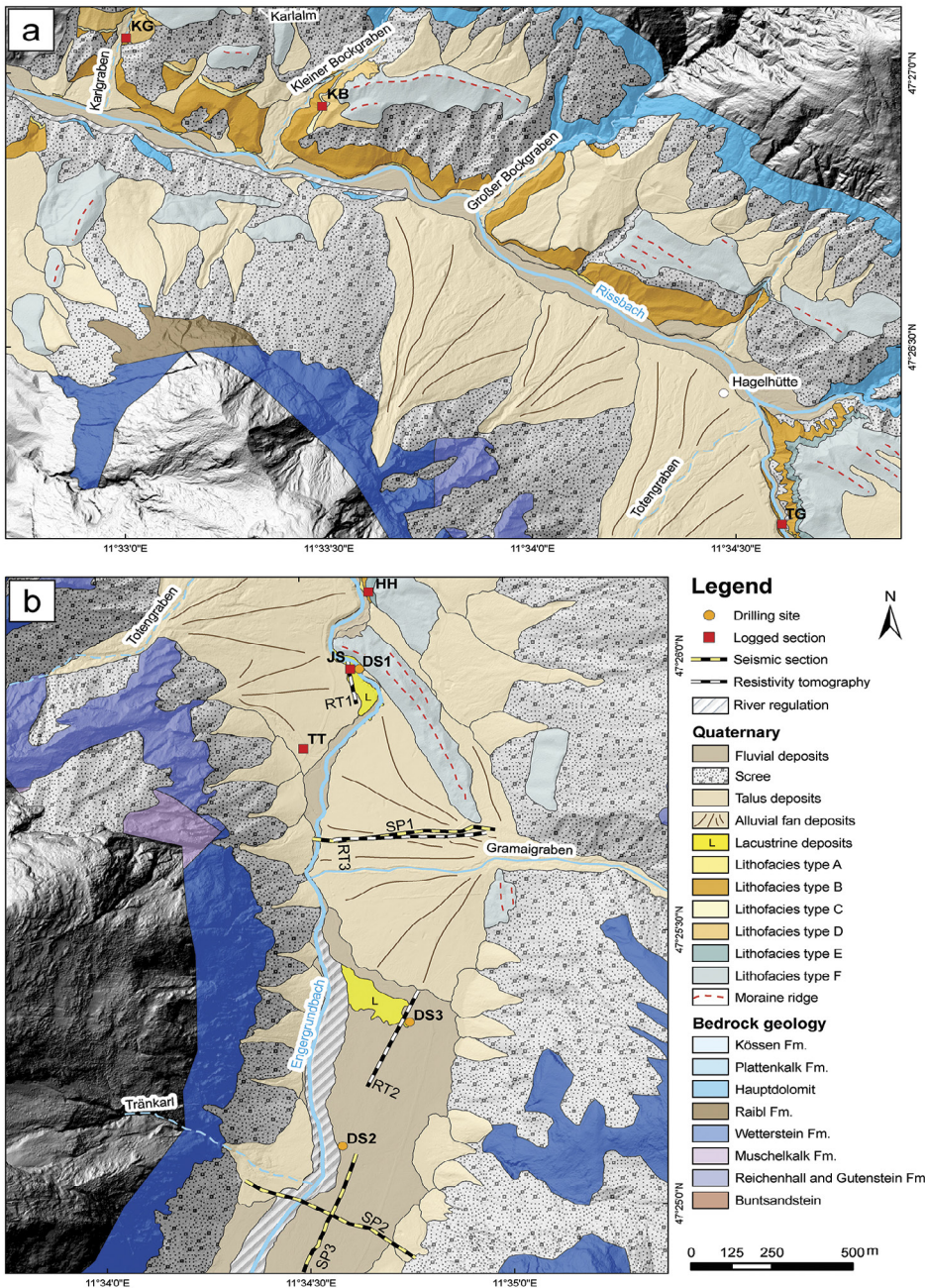
Figure 2: Simplified geological map showing the distribution of Quaternary sediments in the study area. (a) Sedimentary succession between Karlgraben and Hagelhütte in the northwestern part of the central Riss Valley. (b) Map of the northern part of Großer Ahornboden. Basemap: digital terrain model by TIRIS (Source: Land Tirol - data.tirol.gv.at, ©CC BY 3.0 AT). Sections mentioned in the text: KG - Karlgraben, HH - Hagelhütte, KB - Kleiner Bockgraben, JS - Jägerstand, TG - Totengraben, TT- Totengraben trench.

measurements are based on the Wenner geometry proposed by Griffiths and Turnbull (1985) and Griffiths et al. (1990). A 4-point light 10 W high-resolution induced polarization earth resistivity meter (Lippmann Geophysical Instruments) with 60 active electrodes and an electrode spacing of 2.5 m for line RT1, 5 m for profile RT2 and 6 m for RT3 was used. Data acquisition was performed using GeoTest (version 2.42, Rauen Geophysics). The system automatically chooses the appropriate constant current between 1 µA and 100 mA. The inversion and modeling was done using RES2DINV software (version 3.71.113, GEOTOMO SOFTWARE), based on a smoothness-constrained least-squares method including a topographic correction (Sasaki, 1992; Loke and Barker, 1995). The smallest possible cell size for the calculation mesh was used as well as robust data constraints due to the expected high contrast. Contouring of the resulting grid data was done using Natural Neighbour interpolation after Watson (1992).

3.6 Seismic investigation

The seismic survey was performed in order to investigate the thickness and shape of the sediment fill in Großer Ahornboden as well as to determine the bedrock surface. Data acquisition (Summit II system, DMT) was done with 96 (SP1 and SP2) and 48 (SP3) channels (Summit II system, DMT) and a geophone spacing of 6 m. A pneumatic hammer (Vakimpak) was used as a seismic source with a shot interval of 12 m leading to average Common Depth Point (CDP)-fold of 30 traces. The data were processed with ProMAX® (Landmark Graphics Corp.) including standard processing, Automatic Gain Control (AGC), spiking deconvolution, bandpass filter, velocity analysis, Normal Move Out (NMO) correction, Common Depth Point (CDP) stacking, and depth migration for the reflection seismics. To obtain a better image of the nearly vertical flanks of the valley Dip
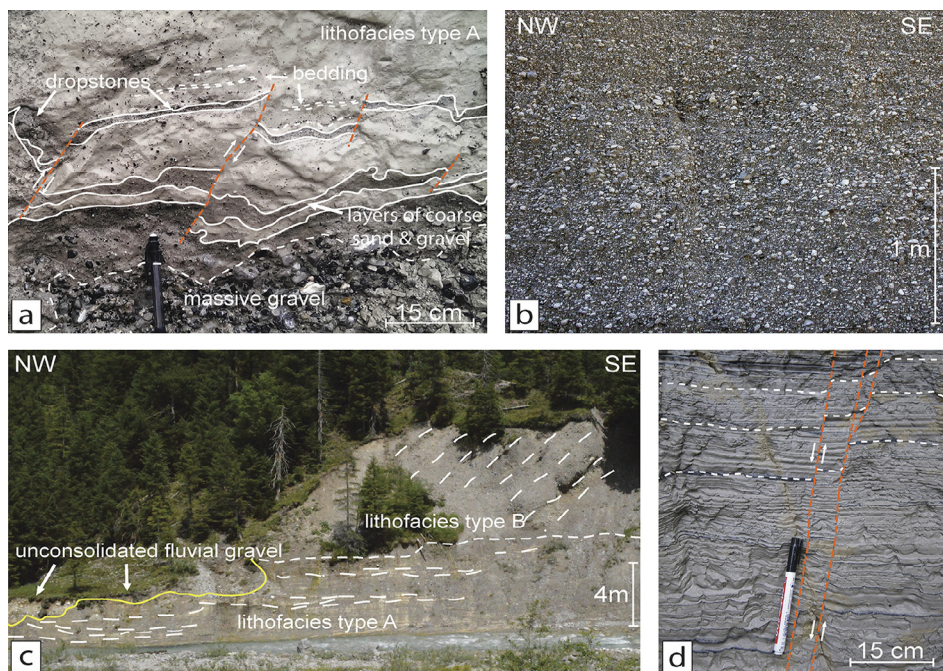
ded by A. Hogg, University of Waikato, was used for the background correction. Ages were calculated according to Stuiver and Polach (1977) using the AMS measured $^{13}C/^{12}C$ ratio which accounts for both natural and machine isotope fractionation. Ages were calibrated using INTCAL13 (Reimer et al., 2013) and the Calib 7.0 software (Stuiver et al., 2013). Calibrated ages are reported with 2σ uncertainties.

3.5 Electrical resistivity tomography (ERT)

Multi-electrode resistivity sounding was used to characterize the sediment fill of Großer Ahornboden (Fig. 2b). The

Figure 3: (a) Lithofacies type A sediments in the Hagelhütte section showing layers of sand and gravel within fine-grained background sediment and dropstones of different sizes. (b) Gravel with sandy matrix forming a sediment cliff at the junction of Hasenbach and Engergrundbach. (c) Delta complex formed by lithofacies A (bottomset) and lithofacies type B (foreset, locally oversteepened) near the entrance of Kleiner Bockgraben. Fluvial gravel of the Rissbach overlies these highly consolidated units with an erosional boundary (yellow line). (d) Regular interbedding of light and dark layers of lithofacies type C sediments with minor faults (orange) in the Karlgraben profile.
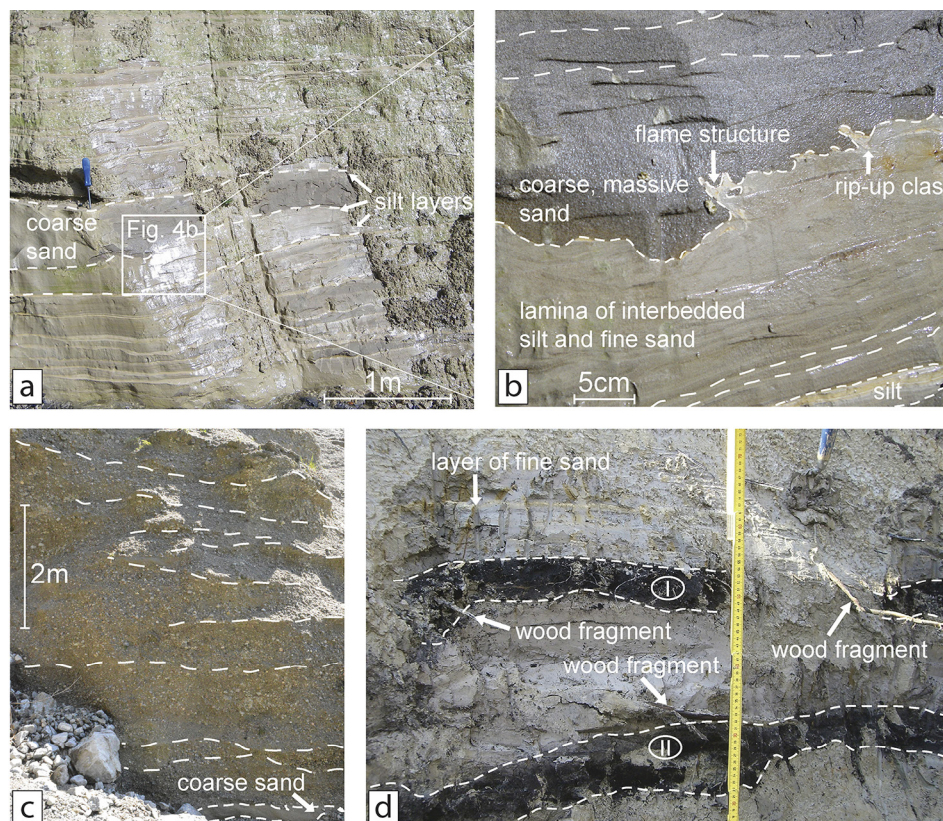

Figure 4: (a) Interbedded sand and silt of lithofacies type D in the Karlgraben profile. (b) Close-up of this section showing an erosive channel-fill with flame structures and rip-up-clasts. (c) Horizontally bedded and partly cemented lithofacies D gravel forming cliffs in the upper part of the Karlgraben profile. (d) Unconsolidated fine grained sediment with two layers of gyttja (I, II) and abundant wood fragments in an outcrop at the DS1 site.

Moveout (DMO) correction instead of the NMO correction was applied. The refraction tomography was calculated with using Rayfract (Intelligent Resources Inc.), which uses the Wavepath Eikonal Traveltime Tomography (WET, Schuster and Qintus-Bosz, 1993) to calculate seismic velocities. The final result is a seismic depth section consisting of a reflection seismic image and the velocity distribution down to a maximum depth of 200 m below surface.

4. Results

4.1 Sediment succession

4.1.1 Lithofacies type A

This unit is exposed between 1032 m (Karlgraben area) and 1095 m a.s.l. (Hagelhütte area), varies in thickness between 1 and 5 m, and comprises yellow to gray, mud-rich calcareous silt and sand containing individual clasts or lenses of angular to sub-rounded dropstones (Fig. 3). Several cm-thick layers of sand and gravel-sized debris also occur. Synsedimentary deformation structures such as flame structures and small-scale faults with vertical offsets of up to 10 cm are common (Fig. 3a). The dropstones are exclusively of local origin and show a high abundance of middle to upper Triassic carbonates (Wetterstein Formation, Hauptdolomit, Plattenkalk), occasional lower Triassic rauhwacke (Reichenhall Formation) and very few Jurassic marlstones.

4.1.2 Lithofacies type B

Gravel with varying sandy matrix overlies lithofacies type A sediments in several locations (Fig. 3b). The fabric is predominantly clast-supported, with
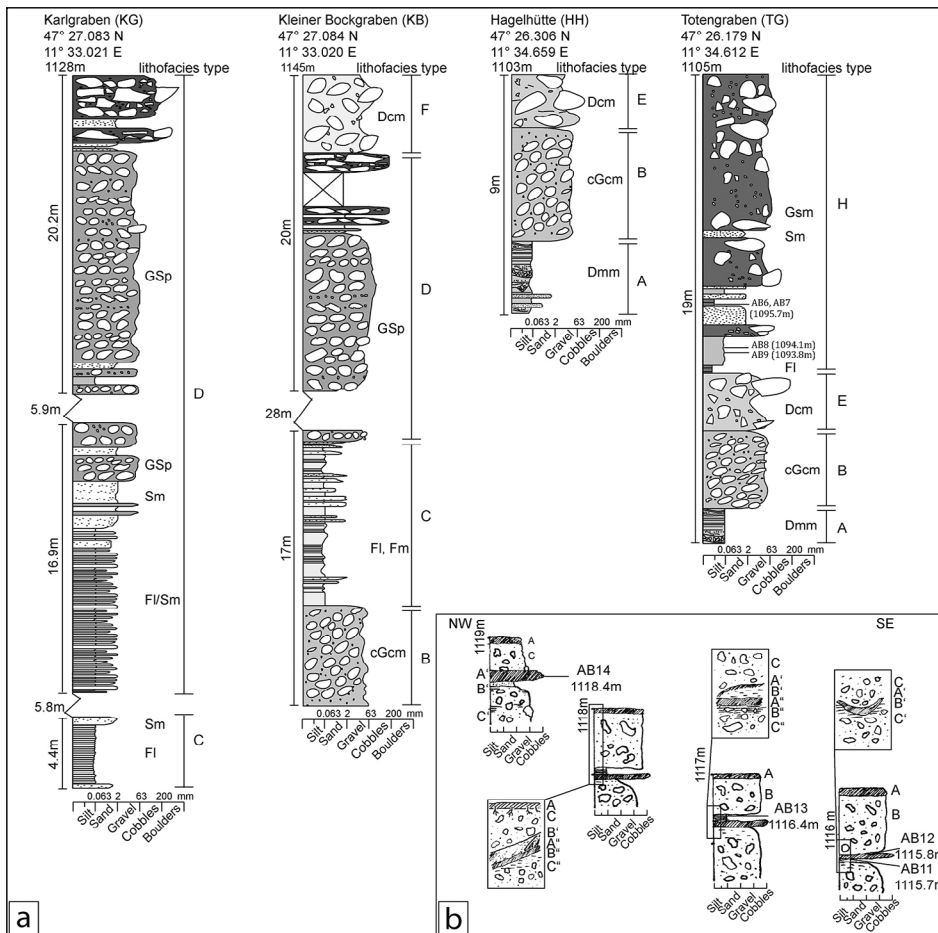
Figure 5: (a) Sedimentary logs of sections in the study area. See Figure 2 for their locations. Abbreviations: Dcm - diamict, clast-supported, massive; Dmm - diamict, matrix-supported, massive; Fm - fine-grained sediment, massive; Fl - fine-grained sediment, laminated; Gcm - gravel, clast-supported, massive; Gc - gravel, clast-supported; GSm - gravel-sand mixture, massive; GSp – gravel-sand mixture, planar bedded; P - peat/gyttja; Sm - sand, massive; (b) Paleosols exposed in a trench of the Totengraben debris-flow fan. Radiocarbon-dated wood fragments are labeled AB.

Sampling Site	Sample	Sampling Elevation (m a.s.l.)	Lab code	14C age BP	Calibrated 14C age BP/AD (2 sigma range)
Outcrop at DS1 11°34.642E, 47°25.985N	AB2	1110	UBA-18807	4691 ±28	5320-5576 cal BP
Profile TG (Fig. 5a) 11°34.612E, 47°26.179N	AB6	1095.7	UBA-20610	3167 ±33	3272-3454 cal BP
	AB7	1095.7	UBA-20611	3150 ±38	3252-3452 cal BP
	AB8	1094.1	UBA-20890	3181 ±25	3365-3449 cal BP
	AB9	1093.8	UBA-20891	3320 ±24	3476-3613 cal BP
Outcrop Engergrundbach 11°34.666E, 47°25.892N	AB10	1108.0	UBA-23253	4643 ±38	5303-5469 cal BP
Profile TT (Fig. 5b) 11°4.454E, 47°25.819N	AB11	1115.7	UBA-23254	398 ±19	335-507 cal BP
	AB12	1115.8	UBA-23255	283 ±27	159-451 cal BP
	AB13	1116.4	UBA-23256	170 ±29	0-289 cal BP
	AB14	1118.4	UBA-23257	285 ±27	287-452 cal BP
DS2, northern Gr. Ahornboden 11°34.752E, 47°25.337N	AB25	1121.4	UBA-26295	161 ±25	1665-1950 AD
	AB26	1120.4	UBA-26296	346 ±27	1465-1636 AD
	AB33	1109.4	UBA-26662	9161 ±48	10232-10486 cal BP
DS1, 11°34.643E, 47°25.985N	AB27	1106.1	UBA-26656	5411 ±47	6021-6300 cal BP
	AB28	1105.1	UBA-26657	7948 ±54	8637-8993 cal BP
	AB29	1103.2	UBA-26658	8386 ±50	9286-9516 cal BP
	AB30	1102.2	UBA-26659	8871 ±50	9768-10180 cal BP
	AB31	1100.7	UBA-26660	8920 ±54	9799-10223 cal BP
	AB32	1099.6	UBA-26661	8941 ±44	9915-10211 cal BP

Table 1: Radiocarbon ages of wood remains.

a varying abundance of striated and keel-shaped clasts. The clast diameter reaches up to 60 mm with a median between 10 and 20 mm, and the clast shape ranges from sub-rounded to sub-angular. Clast lithology is mainly comprised of locally derived middle to upper Triassic carbonates (Wetterstein Formation, Hauptdolomit, Plattenkalk). This unit is typically exposed

as foresets dipping towards NW-NWW (Fig. 3c). Outcrops of this unit can be traced from Karlgraben to Hagelhütte, with the basal part between 1035 and 1095 m a.s.l. and a vertical extension of ~50 m.

4.1.3 Lithofacies type C

These sediments are rhythmically bedded, consisting of clay-rich (up to 12 wt.-%) silt of alternating light and dark grey layers, each typically 0.5 to 1.0 cm thick. 46 such couplets were counted within 60 cm. This lithofacies occurs in Karlgraben and Kleiner Bockgraben (Fig. 5a) only and is characterized by a lack of clasts or dropstones. Normal faults with up to 10 cm displacement are present, similar to lithofacies A and B (Fig. 3d). The basal contact to the underlying unit (lithofacies type B) is sharp. The best exposed outcrop (Kleiner Bockgraben) displays a 5 m-thick layer, with a gradual transition towards silty and sandy sediments in the upper part.

4.1.4 Lithofacies type D

This unit consists of distinctive couplets of several cm-thick, dark grey sand layers and a few mm-thin, yellow to light grey silt layers. 48 such couplets were counted in the lowermost 5 m of this unit in the Karlgraben profile. Minor faults with a few centimeters of displacement, flame structures, convolute bedding and rip-up clasts are common (Figs. 4a, b). The sediment succession shows a coarsening-upward trend expressed by an increase in the relative thickness of the sand layers and a gradual change from fine to coarse sand. This trend continues in upward direction leading to a replacement of the sand by horizontally bedded, sub- to well-rounded and grain-supported gravel with a sandy matrix (Fig. 4c). Cracked clasts are present throughout the upper part of this unit. These sediments crop out in Karlgraben and Kleiner Bockgraben. In the former profile, the unit comprises 11 m of sand and silt couplets and 13 m of gravels, whereas in the latter only 10 m of the succession are exposed.

4.1.5 Lithofacies type E

A diamict comprised of a dark grey silty matrix with gravel- to boulder-sized components, consisting of the same lithologies as the components in the previously mentioned lithofacies ty-
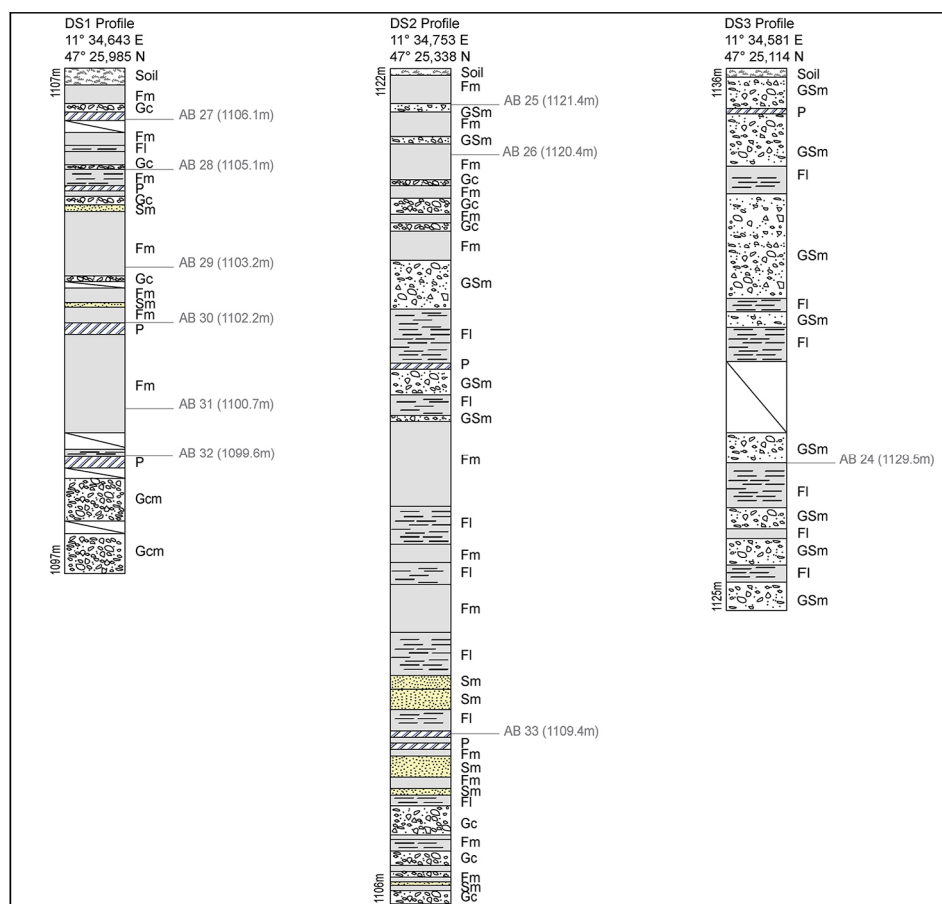
Figure 6: Percussion core logs of DS1, DS2 and DS3. See Figure 2b for their locations and Figure 5 for an explanation of the abbreviations. Radiocarbon-dated samples are labeled AB.

ditional 7 m of this unit further down section (Fig.6). The sediments of this unit are also found near the DS3 drilling site and in the DS3 core.

4.1.8 Lithofacies Type H

Very poorly sorted, angular clasts of local origin, ranging from gravel to boulders, characterize this sediment. Predominantly matrix-supported, the clasts form event layers showing a chaotic fabric. The matrix is composed of brown to greyish silt and less frequently sand. Lithofacies H is typically present within the larger debris-flow fans of the Riss Valley (Fig. 5b). The thickness varies from a few centimeters to several meters. Sediments of this type were found in the DS2 and DS3 cores.

4.2 ¹⁴C data

Only lacustrine and debris-flow sediments (lithofacies units G and H) yielded wood remains suitable for radiocarbon dating. The highly compacted sediments (lithofacies A and B) are devoid of organic matter. A total of 20 samples were radiocarbon-dated and yielded ages between 9161±48 and 161±25 BP (Table 1). Wood remains from the lacustrine sediments of Großer Ahornboden cover the time interval from 9161 ±48 to 4643 ±38 BP (10.5-5.3 cal ka BP), and hence allow to constrain the age and duration of this paleolake. A second and much smaller lake identified by wood-bearing gyttja in the Totengraben section (Fig. 2) yielded ages between 3320 ±24 and 3150 ±33 BP (3.6-3.3 cal ka BP). Finally, the topmost section of the Totengraben alluvial fan contained wood fragments which range from 170 ±29 to 398 ±19 BP, constraining the latest phase of debris-flow deposition and fan aggradation to approximately the 16th to the 19th century AD (Fig. 5b and Table 1).

4.3 Resistivity tomography sections

The RT1 resistivity section starts north of the DS1 site and aimed at tracing the outcropping fine grained sediments in southward direction. The electrode spacing of 2.5 m allowed a good resolution of the uppermost 20 m of the valley fill. The resulting model permits distinguishing between three units of different resistivity values. The upper unit (U1, Fig. 7a) is characterized by values between 45 and 90 Ωm, displays a maximum thickness of up to 12 m and can be traced along the entire 150 m-long profile. A

pes, overlies lithofacies type B in the Hagelhütte and Totengraben (Fig. 5a) sections. Keel-shaped and striated clasts are abundant, but cracked clasts are rare. The sediment is characterized by a poorly sorted texture and varies from clast- to matrix-supported, although the former fabric is more abundant.

4.1.6 Lithofacies type F

This comprises diamictic sediments containing keel-shaped and striated clasts of locally derived lithologies, whose shape ranges from angular to sub-rounded. The components a very poorly sorted and range from gravel to cobbles; rare boulder up to 1 m in diameter are present as well. The clasts occur in a silty to sandy matrix, but are generally clast-supported. The fabric is chaotic, and deformation structures, cracked clasts or any other indications of strong compaction are missing. This lithofacies unit forms the uppermost part of the succession at Hagelhütte and in Karlgraben and Kleiner Bockgraben (Fig. 5a).

4.1.7 Lithofacies type G

These sediments comprise well bedded, light to dark grey, calcareous silts. In contrast to the sediments discussed above, no evidence of consolidation was observed. Several gyttja layers containing wood fragments are present within the uppermost 3 m (Fig. 4d), especially near DS1. Core DS1 provides ad-
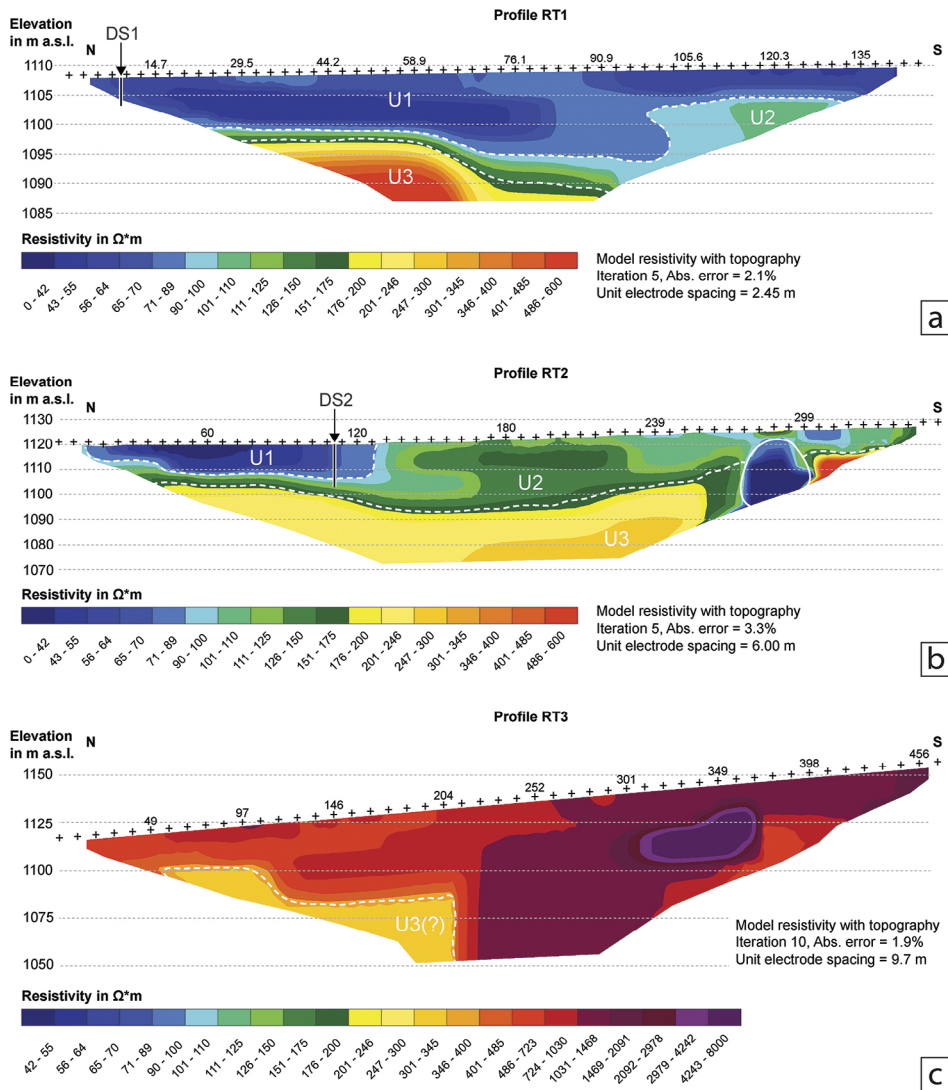
Figure 7: Earth resistivity tomography (ERT) profiles RT1, RT2 and RT3. See Figure 2b for their locations. Electrode positions are indicated by crosses and numbers. The sediment units (U1 to U3) mentioned in the text are indicated by dotted white lines. The area affected by the power line in the south of profile RT2 is highlighted by a solid white line.

4.4 Seismic sections

Seismic refraction and reflection analyses resulted in a subsurface stratigraphy model (Figs. 8a, b, c) for the sediment fill and the bedrock beneath. The deepest refractor and the strongest reflector in all seismic profiles occurs at a depth of around 140 m in the center of the valley. In profiles SP1 und SP2 this refractor rises to the surface at the start and end of the profiles giving rise to a U-shape cross section. Because of the influence of the Gramai debris-flow fan this boundary is not clearly visible at the eastern end of SP1. Refraction velocities of 4300-5100 m/s suggest disjointed carbonate rocks as the bedrock (Bader, 1979; Hoffmann and Schrott, 2003; Sass, 2007). The sediment fill of SP2 and SP3 shows uniform layering. The uppermost layer with velocities near 550 m/s and a maximum thickness of 10 m following the present-day topography indicates unconsolidated gravel or sand. The underlying layer with an average velocity of 950 m/s and a maximum thickness of 15 m points to more dense gravel or sand. The sediment layer below 25 m depth with velocities of 2750

m/s and a thickness of up to 115 m indicates consolidated deposits. Till deposits can be excluded, because resistivity values close to 300 Ωm were recorded in the nearby ERT profile RT2 (cf. Sass, 2007).

The interpretation of the sediment fill at SP1 is more complicated, because the tributary at the Gramaigraben builds a large debris-flow fan in this area. Deeper reflection horizons and the partitioning of the overlying refraction layer indicate that the valley is filled with sediments from the east. Nevertheless, layers comparable to those in profile SP2 are present as well. Again, the uppermost two layers with velocities near 550 and 1100 m/s, respectively, which have a combined thickness of 20 m, consist of unconsolidated gravel or sand. The layer beneath shows velocities near 2200 m/s in the west and near 2400 m/s in the east and reaches a maximum thickness of 70 m, probably representing consolidated deposits. The velocity distribution indicates more fine-grained sediment in the western and coarser material in the eastern part, the latter being part of the

thin Unit 2 (U2) with higher resistivity is present in the southern part of the profile. Unit 3 (U3) shows significantly higher resistivity values than U1 and U2 (>300 Ωm) and its upper boundary is sharp and dips slightly southward. South of the Gramai fan the RT2 section shows a similar structure in the subsurface (Fig. 7b). Calculated resistivity values for U1 range between 20 and 90 Ωm, strikingly similar to RT1. The thickness of U1 is between 10 and 20 m and can be traced for 150 m southward. Unit 2 is more heterogeneous and borders U1 to the south with resistivity values between 100 and 200 Ωm. Sediments characterized by resistivity values between 150 and 300 Ωm (U3) are present beneath both U1 and U2. The low resistivity dome in the south (highlighted in Fig. 7b) is attributed to an electrical power line. The RT3 section (Fig. 7c) generally shows very high resistivity values along the whole profile which are caused by the deposits of the Gramai debris-flow fan. In the northern part the resistivity values are lower at greater depth which suggests the presence of Unit 3 (U3).

Gramai debris-flow fan. The deepest layer with velocities near 2650 m/s and a maximum thickness of 80 m is comparable to the deepest layer of SP2 and SP3 and represents consolidated deposits. Both deeper layers were probably formed by valley sediments interfingering with lateral debris-flow or talus deposits.

5. Discussion

5.1 Sediment succession and morphology of the central Riss Valley

Lithofacies type A and B sediments (as described in chapter 4) are present throughout the central Riss Valley and are interpreted as bottomset and foreset of a proglacial, (glacio) lacustrine deltaic complex (or a series of lateral delta bodies) as indicated by the abundance of dropstones and striated as well as keel-shaped clasts. These sediments therefore record a perennial lake that occupied the Riss Valley during the deglaciation and/or the Lateglacial. Similar sediments of the bottomset facies (thick diamictic silts) are present in the northern Riss Valley (Spötl et al., 2014) as well as in the Isar Valley suggesting that this lake extended beyond the Riss Valley. No absolute age constraints are currently available for this lower, overcompacted succession neither in the Riss nor in the Isar Valley due to the complete lack of organic material.

The foreset gravels are sharply overlain by laminated clayey silts of a younger bottomset (lithofacies type C) providing evidence of a rapid drowning of these delta complexes due to a rise in lake level. These sediments and the associated coarsening-upward succession also witnessed overconsolidation.

5.2 Bedrock geometry and valley-fill at Großer Ahornboden

The seismic reflector delineates the up to 140 m-deep buried bedrock surface as a sharp and continuous boundary with steeply inclined flanks and a concave shape. The refraction seismic velocity model is consistent with the interpretation of the basal reflection as the top of the bedrock. The textbook-like U-shaped bedrock surface geometry underscores glacier erosion as the key process forming this depression (Benn and Evans, 2010; Cook and Swift, 2012). The overlying sediments display no internal reflections, but the velocity analysis allows distinguishing a shallow upper part with p-wave velocities of 500 to 1100 m/s from a thicker, lower unit with higher velocities. ERT data (RT2) confirm this division, showing low resistivity values (< 175 Ωm) in the overlying sediment in contrast to increased resistivity values below 1090 m a.s.l., ranging from 200 to 500 Ωm, corresponding
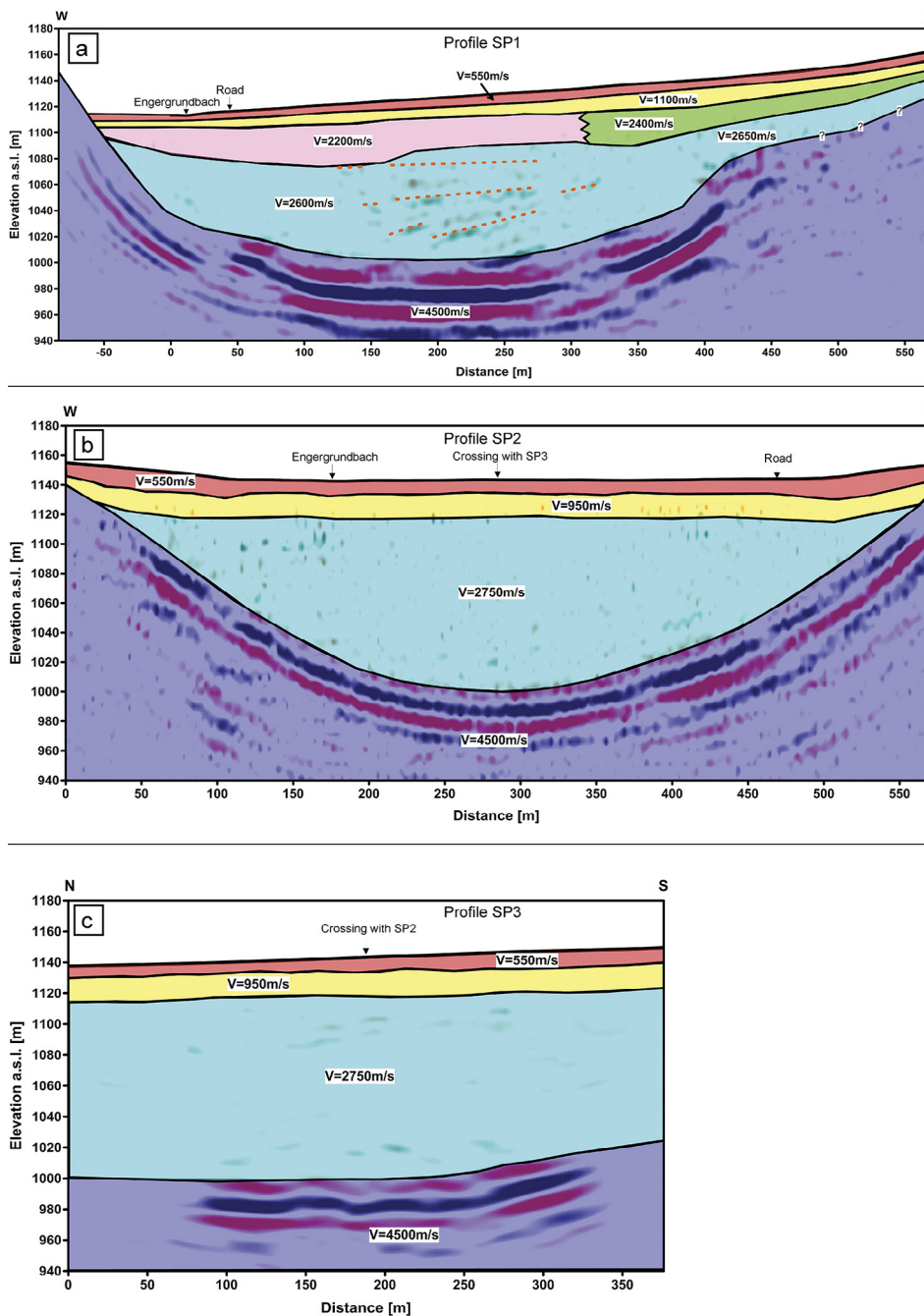

Figure 8: Joint reflection and refraction seismic sections: reflection seismic data are displayed as amplitude plot while refraction seismic units are color-coded and their mean p-wave velocities are indicated.

to higher p-wave velocities (2750 m/s). The seismic units can be traced throughout Großer Ahornboden, although the subsurface of the Gramai alluvial fan suggests more complex internal structures. SP1 reveals a series of west-dipping reflections, interpreted as aggradation surfaces of the paleo-Gramai fan.

The lower sediment package identified by geophysical data might represent an older valley-fill, which became overconsolidated by a later ice advance or sediment overburden (see section 5.3). This agrees with seismic data from southern Bavaria including the Isar Valley, which revealed a seismic bipartition into a lower and an upper sediment unit, distinguished by their high and low p-wave velocities, respectively (Bader, 1979). Such a bipartite valley fill is found in many glacially carved valleys (e.g. Brückl et al., 2010; Preusser et al., 2010).

The upper sediment unit at Großer Ahornboden, apart from the lacustrine fine-grained sediments discussed in section 5.4, represents a heterogeneous valley-fill probably consisting of fluvial deposits with interfingering debris-flow layers and rockfall debris derived from the oversteepened mountain flanks.

5.3 Lateglacial sedimentation

Despite the absence of chronological data some constraints can be placed on the depositional history by comparison with similar successions in other valleys (e.g. Reitner, 2007; Reitner et al., 2010). The last phase of glacial overdeepening most likely occurred during the LGM, when the area was covered with ice up to 2100 m a.s.l. (Fig. 9a; Wolf, 1922; van Husen, 1987), eroding the bedrock beneath the Großer Ahornboden to its present level and shape. During the ice decay large parts of the Riss valley were filled by a lake (Figs. 9b, 10a), most lost likely dammed by the stagnant Isar-Loisach ice body. Thick sediments of the central Riss Valley were deposited in this lake. Subsequent glacier oscillation (Figs. 9c, 10b) resulted in sediment overconsolidation north of Großer Ahornboden (similar to the Windau and Drau valleys - Reitner, 2007). During ice-free periods substantial amounts of sediment were deposited at Großer Ahornboden. Cirque glaciers re-advanced during Lateglacial stadials, compacted the sediments at Großer Ahornboden and left behind moraine ridges in the southern part of the valley (Figs. 9d, 10c). Unfortunately, the age of these features is unknown, due to the lack of boulders suitable for exposure age dating (H. Kerschner, pers. comm.). Remnants of these sediments (lithofacies type E) are present, for example, at the Karlalm or at the junction with the Laliderer Valley. The best preserved southernmost moraine ridge, stretching half across the valley, dammed the Ahornboden lake during the first half of the Holocene, in combination with the Totengraben debris-flow fan giving rise to the present-day landscape (Figs. 10d, 11a).

5.4 Ahornboden lake phase

Penck (1922) was the first to recognize lacustrine deposits in the inner Riss Valley. Later, Sommerhoff (1971) mentioned lake

sediments at the northern rim of Großer Ahornboden, south of a moraine ridge. Czell et al. (1966) mapped loam in particular in the area of our section DS3 as part of a soil study. We identified lithofacies type G sediments (see section 3.2) outcropping at DS1 and DS2, which confirms the observations by Czell et al. (1966). Correlating the DS1 and DS2 sites is difficult, because they are separated by the Gramai fan. The ERT profile RT1, however, confirms an 8 m-thick lacustrine sediment layer (with low resistivity values <100 Ωm) extending from DS1 to the south. The seismic section SP1 at the Gramai fan does neither indicate nor contradict lacustrine sediments (with interbedded coarser-grained sediments). RT3 provides a hint for the existence of such a layer between 1100 m and 1075 m a.s.l. DS2 and RT2 allow tracing lacustrine sediments to approximately 250 m south of the Gramai fan, but show no evidence of fine-grained sediments in the southern part. Previous models of a lake occupying the entire Große Ahornboden (Czell et al., 1966; Sommerhoff, 1977) are therefore incorrect.

The base of the lacustrine silts was reached at the DS1 at 1099 m a.s.l. Wood remains constrain the onset of the lake phase to 10.5-10.2 cal ka BP (Table 1). The end of the lacustrine sedimentation occurred at 5.5-5.3 cal ka BP as constrained by wood fragments in the uppermost 20 cm of the well-bedded clayey silts.
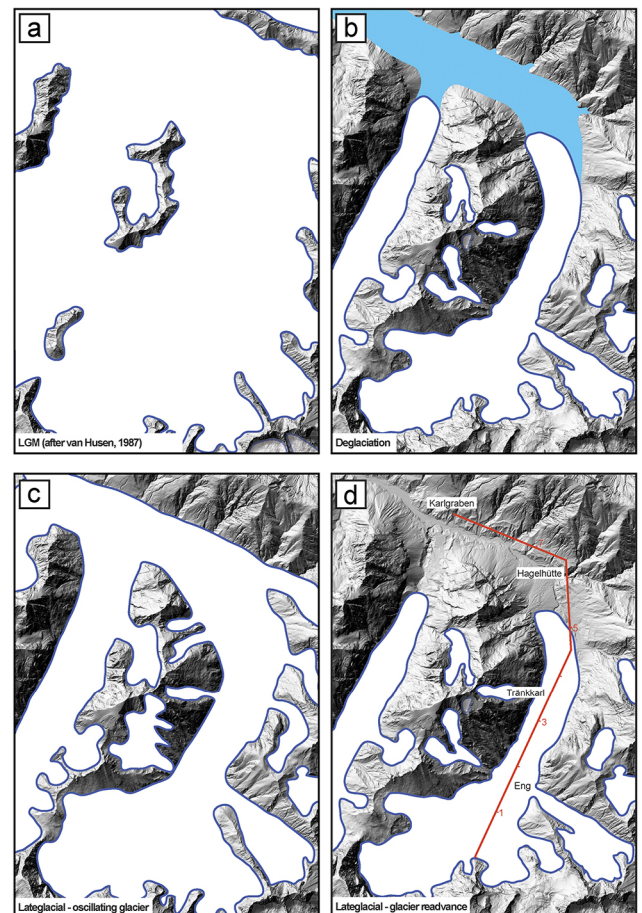

Figure 9: (a-d) Paleogeographical sketch maps illustrating the evolution of the study area between the LGM and the Lateglacial. The trace of Figure 10 is indicated. Basemap: digital elevation model by TIRIS (Source: Land Tirol - data.tirol.gv.at, ©CC BY 3.0 AT).
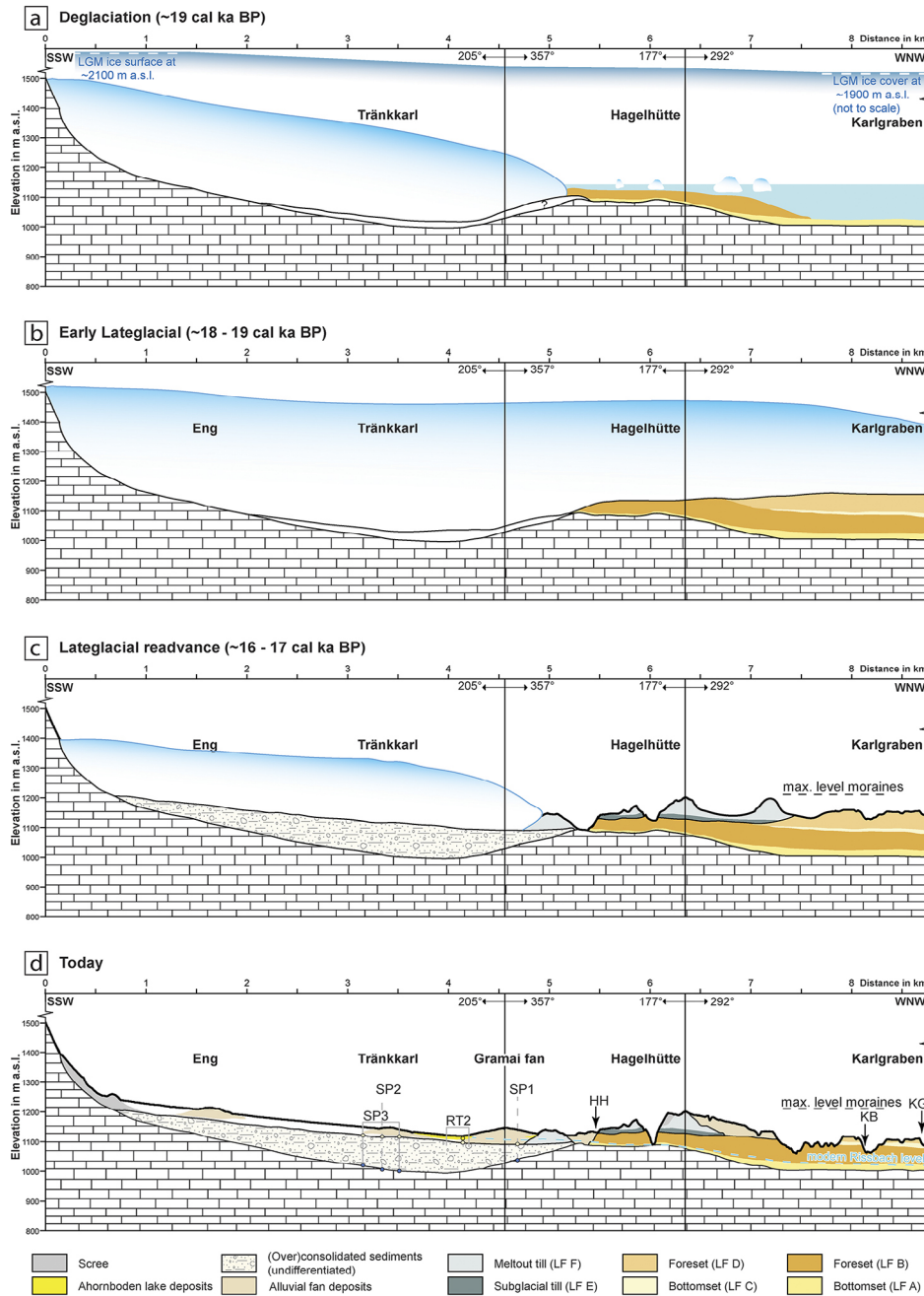
Figure 10: (a-d) Schematic longitudinal section showing the glacial and depositional evolution of the inner Riss Valley between the end of the LGM and the present-day (for profile trace see Fig. 9d). Abbreviations refer to sediment profiles (Fig. 5), resistivity tomographies (section 4.3) and seismic surveys (section 4.4).

remains from the distal part of this fan (see profile TG, Fig. 5), found within thin silt beds at 1094 m a.s.l., i.e. lower than the base of the Ahornboden lake sediments, yielded ages of 3.6-3.3 cal ka BP. This lacustrine interval was subsequently buried beneath several meters of debris-flow gravel indicating that until about 3.6 cal ka this fan was significantly smaller than today (Figs. 11b, 11c).

6. Conclusions

Seismic data confirm the glacial origin of the inner Riss Valley and revealed the presence of two distinct sediment units. The thick lower unit shows high p-wave velocities and is interpreted as Lateglacial clastic sediments, which became overcompacted during subsequent ice advances, whereas the thinner upper succession shows low seismic velocities and did not experience glacial compaction. The older sediments are well exposed along the central Riss Valley and can be correlated to overcompacted bottomset silts in the subsurface of the Isar Valley. Logging of these sediments revealed two coarsening-upward sequences of advancing delta bodies separated by a sharp unconformity. The lower unit is attributed to lacustrine conditions during the deglaciation, whereas the upper one probably reflects sedimentation in response to re-advances of local glaciers during the early Lateglacial. A lake formed in the northern part of today´s Großer Ahornboden ceased to exist 5.5-5.3 ka cal BP.

Acknowledgements

The most likely candidate for damming this former lake is the moraine ridge near DS1 in combination with the prograding Totengraben fan (Fig. 11b). The top of the ridge presently reaches up to 1135 m a.s.l. and it is likely that – subsequent erosion taking into account – its original height was close to 1140 m a.s.l. If filled up to the crest of this ridge, the lake would have stretched as far south as the small fan from Tränkkarl (DS3 site). The western segment of the Lateglacial dam was buried beneath the debris-flow fan of Großer Totengraben. The progradation of this sediment body most likely blocked the channel of Engergrundbach resulting in the formation of a lake. Wood
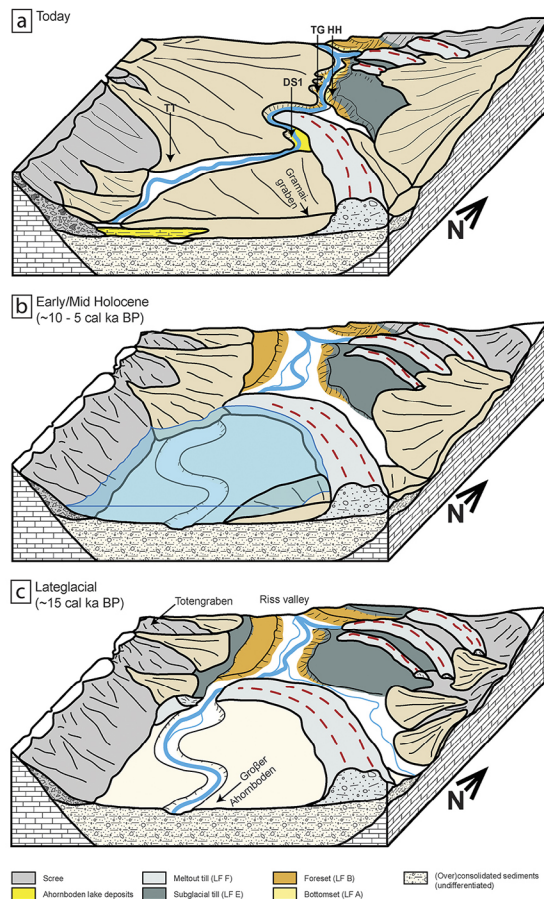
Figure 11: Schematic sedimentation model at the northern rim of Großer Ahornboden.

sity of Innsbruck assisted in the field during the geophysical surveys. Gerhard Doppler, Jürgen Reitner and an anonymous reviewer provided thorough reviews, which improved the clarity of the article.

References

Ampferer, O., 1903. Geologische Beschreibung des nördlichen Theiles des Karwendelgebirges. Jahrbuch der k. u. k. geol. Reichsanstalt, 53, 169-251.

Bader, K., 1979. Exarationstiefen würmeiszeitlicher und älterer Gletscher in Südbayern. Eiszeitalter und Gegenwart, 29, 49-61.

Benn, D.I., Evans, D.J.A., 2010. Glaciers and Glaciation. 2nd ed., 802 p., London (Arnold).

Brückl, E., Brückl, J., Chwatal, W., Ullrich, C., 2010. Deep alpine valleys: examples of geophysical explorations in Austria. Swiss Journal of Geosciences, 103, 329-344. http://dx.doi.org/10.1007/s00015-010-0045-x

Cook, S.J., and Swift, D.A., 2012. Subglacial basins: Their origin and importance in glacial systems and landscapes. Earth-Science Reviews, 115, 332-372. http://dx.doi.org/10.1016/j.earscirev.2012.09.009

Czell, A., Schiechtl, H.M., Stauder, S., Stern, R., 1966. Erhaltung des Naturschutzgebietes ,Großer Ahornboden' durch tech-

nische und biologische Maßnahmen. Jahrbuch Verein zum Schutze der Alpenpflanzen und -Tiere e.V., 31, 33-56.

Frank, H., 1979. Glazial übertiefte Täler im Bereich des Isar-Loisach-Gletschers. Eiszeitalter und Gegenwart, 29, 77-99.

Griffiths, D.H. and Turnbull, J., 1985. A multi-electrode array for resistivity surveying. First Break, 3/7, 16-20. http://dx.doi.org/10.3997/1365-2397.1985013.

Griffiths, D.H., Turnbull, J., Olayinka, A.I., 1990. Two-dimensional resistivity mapping with a computer-controlled array. First Break, 8/4, 121-129, http://dx.doi.org/10.3997/1365-2397.1990008.

Heiri, O., Koinig, K.A., Spötl, C., Barrett S., Brauer, A., Drescher-Schneider, R., Gaar, D., Ivy-Ochs, S., Kerschner, H., Luetscher, M., Moran, A., Nicolussi, K., Preusser, F., Schmidt, R., Schoeneich, P., Schwörer, C., Sprafke, T., Terhorst, B., Tinner, W., 2014. Palaeoclimate records 60-8 ka in the Austrian and Swiss Alps and their forelands. Quaternary Science Reviews, 106, 186-205. http://dx.doi.org/10.1016/j.quascirev.2014.05.021

Hinderer, M., 2001. Late Quaternary denudation of the Alps, valley and lake fillings and modern river loads. Geodinamica Acta, 14/4, 231-263. http://dx.doi.org/10.1016/S0985-3111(01)01070-1

Hoffmann, T., Schrott, L., 2002. Modelling sediment thickness and rockwall retreat in an Alpine valley using 2D-seismic refraction (Reintal, Bavarian Alps). Zeitschrift für Geomorphologie, Suppl. Bd. 127, 153-173.

Hogg AG, Fifield LK, Turney CSM, Palmer JG, Galbraith R, Baillie MGL. 2006. Dating ancient wood by high sensitivity liquid scintillation counting and accelerator mass spectrometry – pushing the boundaries. Quaternary Geochronology, 1/4, 241-248. http://dx.doi.org/10.1016/j.quageo.2006.11.001

Loke, M.H., Barker, R.D., 1995. Least-squares deconvolution of apparent resistivity. Geophysics, 60/6, 1682-1690. http://dx.doi.org/10.1190/1.1443900

Mutschlechner, G., 1948. Spuren des Inngletschers im Bereich des Karwendelgebirges. Jahrbuch der Geologischen Bundesanstalt, 93, 155-206.

Penck, A., 1922. Die Terrassen des Isartales in den Alpen. Ablagerungen und Schichtstörungen der letzten Interglazialzeit in den nördlichen Alpen. Sitzungsberichte Preussischen Akademie der Wissenschaften, physikalisch-mathematische Klasse, 19/20, 182-208.

Preusser, F., Reitner, J.M., Schlüchter, C., 2010. Distribution, geometry, age and origin of overdeepened valleys and basins in the Alps and their foreland. Swiss Journal of Geosciences, 103/4, 407-426. http://dx.doi.org/10.1007/s00015-010-0044-y

Reimer, P. J., Bard, E., Bayliss, A., Beck, J. W., Blackwell, P. G., Bronk Ramsey, C., Grootes, P. M., Guilderson, T. P., Haflidason, H., Hajdas, I., Hatté, C., Heaton, T. J., Hoffmann, D. L., Hogg, A. G., Hughen, K. A., Kaiser, K. F., Kromer, B., Manning, S. W., Niu, M., Reimer, R. W., Richards, D. A., Scott, E. M., Southon, J. R., Staff, R. A., Turney, C. S. M., and van der Plicht, J. (2013). IntCal13 and Marine13 radiocarbon age calibration curves

0-50,000 years cal BP. Radiocarbon, 55/4, 1869-1887. http://dx.doi.org/10.2458/azu_js_rc.55.16947

Reitner, J.M., 2007. Glacial dynamics at the beginning of Termination I in the Eastern Alps and their stratigraphic implications. Quaternary International, 164-165, 64-84._http://dx.doi.org/10.1016/j.quaint.2006.12.016

Reitner, J.M., Gruber, W., Römer, A., Morawetz, R., 2010. Alpine overdeepenings and palaeo-ice flow changes: an integrated geophysical-sedimentological case study from Tyrol (Austria). Swiss Journal of Geosciences, 103/3, 385-405. http://dx.doi.org/10.1007/s00015-010-0046-9

Sasaki, Y., 1992. Resolution of resistivity tomography inferred from numerical simulation. Geophysical Prospecting, 40/4, 453-464. http://dx.doi.org/10.1111/j.1365-478.1992.tb00536.x

Sass, O., 2007. Bedrock detection and talus thickness assessment in the European Alps using geophysical methods. Journal of Applied Geophysics, 62, 254-269.

Schrott, L., and Sass, O., 2008. Application of geophysics in geomorphology: Advances and limitations exemplified by case studies. Geomorphology 93/1-2, 55-73. http://dx.doi.org/10.1016/j.geomorph.2006.12.024

Schuster, G.T., Quintus-Bosz, A., 1993. Wavepath eikonal traveltime inversion: Theory. Geophysics, 58/9, 1314-1323 http://dx.doi.org/10.1190/1.1443514

Sommerhoff, G.,1977. Zur spät- und postglazialen Morphodynamik im oberen Rißbachtal, Karwendel. Mitteilungen der Geographischen Gesellschaft München, 62, 89-103. http://dx.doi.org/10.1016/j.jappgeo.2006.12.003

Sperazza, M., Moore, J.N. and Hendrix, M.S., 2004. High-resolution particle size analysis of naturally occurring very fine-grained sediment through laser diffractometry. Journal of Sedimentary Research, 74/5, 737-743. http://dx.doi.org/10.1306/031104740736

Spötl, C, Mair, D., Starnberger, R., 2014. From Vorderriß to Großer Ahornboden: Quaternary geology of the Riss Valley (Karwendel Mountains), In: From the Foreland to the Central Alps (ed. by H. Kerschner, K. Krainer and C. Spötl), DEUQUA Excursion Guide, 32-44, Berlin (Geozon). http://dx.doi.org/10.3285/g.00011

Stuiver, M. and Polach, H.A., 1977. Reporting of ^{14}C data. Radiocarbon, 19/3, 355-363.

Stuiver, M, Reimer, PJ, Reimer, RW., 2013. CALIB 7.0. (WWW program and documentation). http://calib.qub.ac.uk/calib. (accessed on 24 November 2015)

van Husen, D., 1987. Die Ostalpen in den Eiszeiten. Veröffentlichung der Geologischen Bundesanstalt 2, 24 pp.

van Husen, D., 2000. Geological processes during the Quaternary. Mitteilungen der Österreichischen Geologischen Gesellschaft, 92, 135-156.

Watson, D.F., 1992. Contouring - A guide to the analysis and display of spatial data. Pergamon, 321 pp.

von Wolf, H., 1922. Beiträge zur Kenntnis der eiszeitlichen Vergletscherung des Achenseegebietes in Tirol. Mitteilungen der Geographischen Gesellschaft München, 15, 147-304.

David MAIR[1)*], Werner CHWATAL[2)], Paula J. REIMER[3)] & Christoph SPÖTL[4)]

[1)] Institute of Geology, University of Innsbruck, Innrain 52, 6020 Innsbruck, Austria, Present address: Institute of Geological Sciences, University of Bern, Baltzerstrasse 1+3, 3012 Bern, Switzerland;

[2)] Department of Geodesy and Geoinformation, TU Wien, Gusshausstr. 27-29, 1040 Vienna, Austria;

[3)] Centre for Climate, the Environment and Chronology (14CHRONO), School of Natural and Built Environment, Queen's University Belfast, Belfast BT7 1NN, UK;

[4)] Institute of Geology, University of Innsbruck, Innrain 52, 6020 Innsbruck, Austria;

[*)] Corresponding author: david.mair@geo.unibe.ch